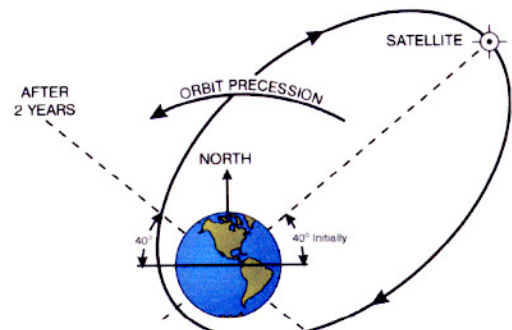
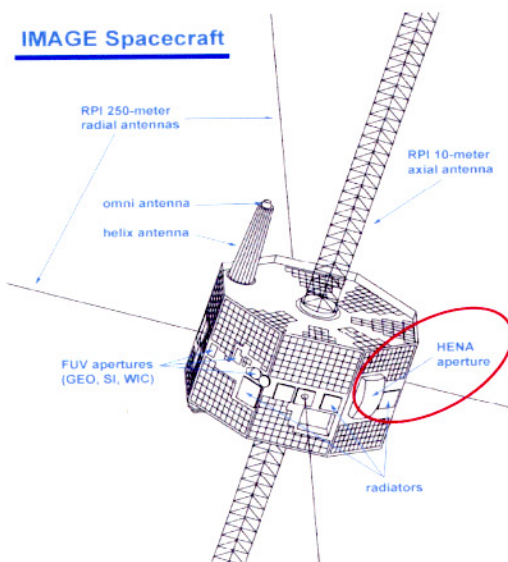


IMAGE衛星によるRingCurrent観測

吉田 大紀 (京大・理)

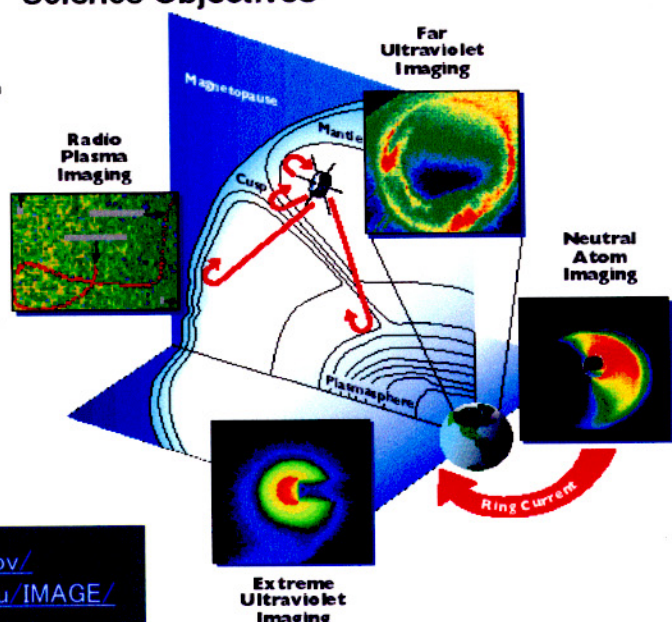


- 1 spin 2分
- 1 pass 14.2時間
- spin軸は軌道面に垂直
- 2000年3月25日 打ち上げ

IMAGE Science Objectives

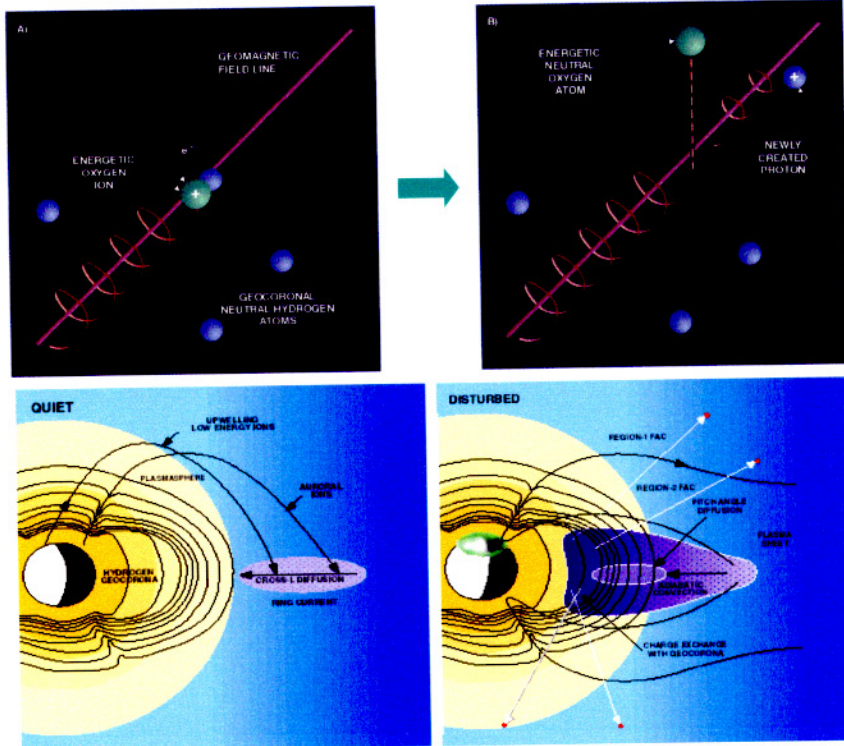
- 1) What are the dominant mechanisms for injecting plasma into the magnetosphere on substorm and magnetic storm time scales?
- 2) What is the directly driven response of the magnetosphere to solar wind changes?
- 3) How and where are magnetospheric plasmas energized, transported, and subsequently lost during storms and substorms?

The IMAGE mission addresses these objectives in unique ways using imaging techniques.



Neutral Atom Imaging

- ・高エネルギーイオンと中性粒子(ジオコロナ)の荷電交換でENAが発生
 - ・高エネルギーイオンの密度、分布函数、ジオコロナの密度に依る
 - ・視線方向の積分値で観測



ENAデータプロット

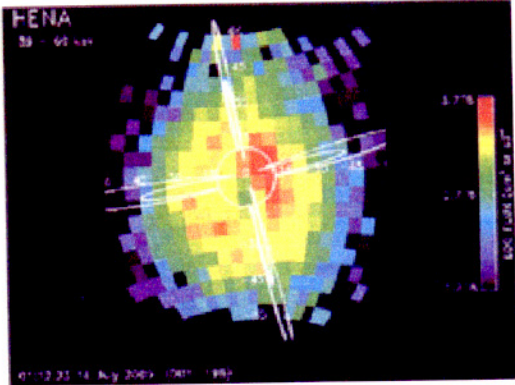
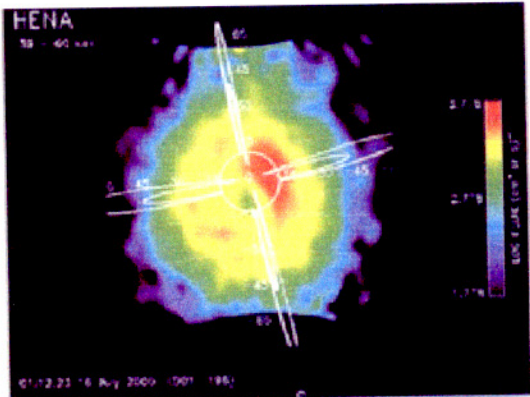
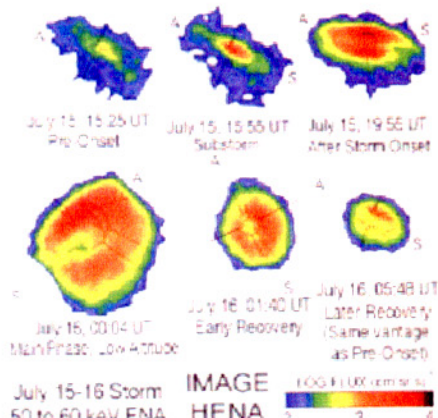


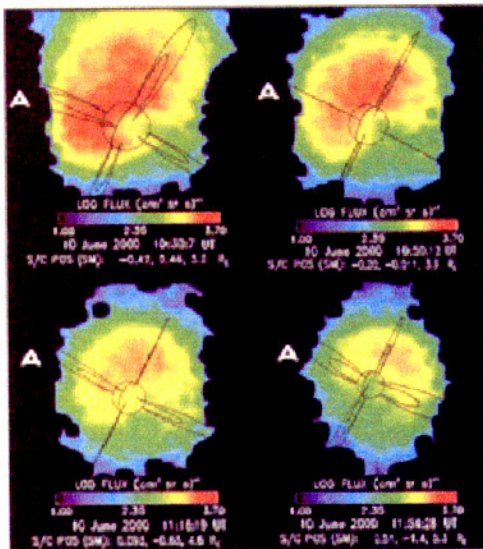
Figure 1. HENA ENA ring current emission 0112UT July 16, 2000. (a) Image from above the Earth's north pole. This vantage point provides a fairly undistorted view of the local time distribution of ENA emission. (High pixel fluxes along the top edge result from an instrument artifact.) (b) Same data as (a), in array of pixel values. (c) Same as (a), but pixels are smoothed.

- ・白線 … $L = 4\text{Re}$ 及び 8Re
00, 06, 12, 18 LT
 - ・A … Anti-Sunward
 - ・S … Sunward
 - ・N … Noon

2000/07/15 – 16 Event

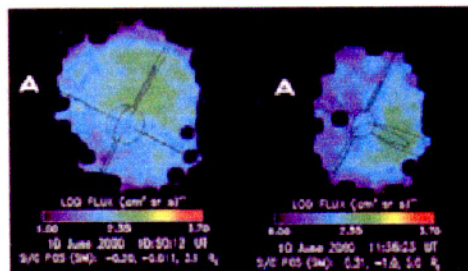


① **Figure 2.** Images from the July 15, 16 2000 storm. This 14 hour sequence covers an entire orbit, so the distance from Earth and viewing perspective varies greatly. In each instance, the brightest emission stems from low altitude mirroring ions that charge exchange in the dense low altitude exosphere.



① **Figure 3.** Sequence of images from June 10, 2000 storm of ENA emission at 16 to 27 keV (assuming hydrogen). Although the spacecraft moves within its orbit over the 1.5 hours covered by this sequence, the viewing perspective changes little enough that the gradient/curvature drift of the parent ion population can be followed. Over this period, the pattern rotates clockwise about the Earth by $\sim 90^\circ$. The rectangular scallops along the edges of some images are smoothing artifacts equal in linear dimension to 2 adjacent pixels (roughly the size of two pixels at this energy). Peak pixels contain about 100 counts.

Fig. 3 ..
 • 16~27 keV
 • 90分で90度drift .. 1周6時間
 ↓
 Shultz and Lanzerotti [1974] (20 keV Proton)
 • L ~ 7Re のdrift周期
 ↓
 これを参考に.. 40 keVなら、1周約3時間
 ↓
 Fig. 4 ..
 • 39~50 keV
 • 45分で90度drift これも一致

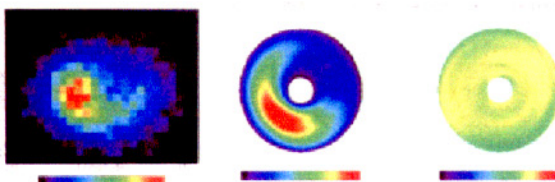


① **Figure 4.** Two images from June 10, 2000 storm of ENA emission at 39 to 50 keV, assuming hydrogen atoms dominate. Over the 45 minute period between these images, the pattern rotates clockwise about the Earth by about 90° .

- Bastille .. 3~4Re
- 2000/06/10 .. 6~8Re にピーク

2000/06/10 Event

Example of Deconvolution of HENA Image at 21.5 keV on 6/10/00



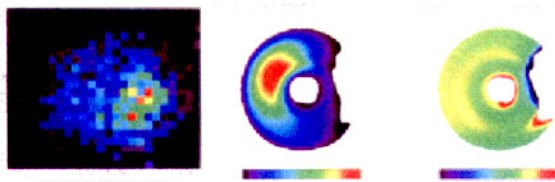
2000/06/10 Event 2

左 .. データ pixel $6^\circ \times 6^\circ$

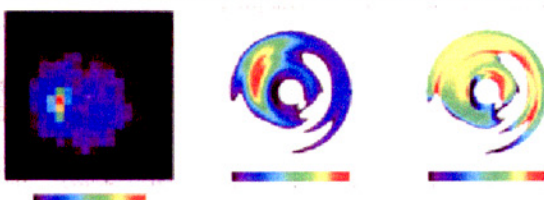
中 .. equatorial ion flux integrated over pitch angle

右 .. Jpara (negative) or Jperp (positive)

Example of Deconvolution of HENA Image at 44.5 keV on 6/10/00



Example of Deconvolution for Small HENA Image on 6/10/00



④

Fig. 1 Examples of equatorial pitch angle distributions extracted from HENA images. See text for description and interpretation of images.

- a) と b) の間
- c) と d) の間に injection
- radiation belt 内は観測なし

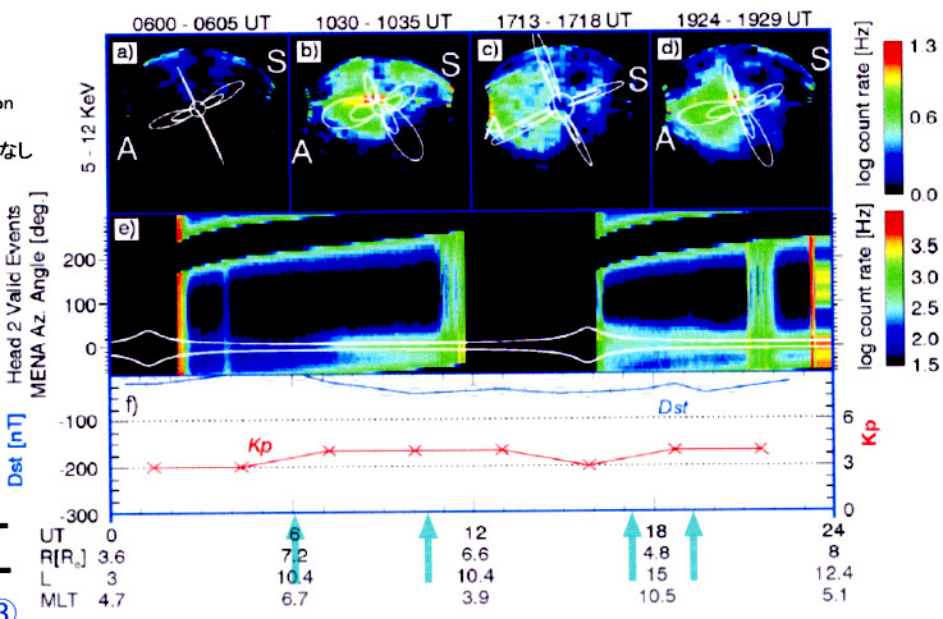
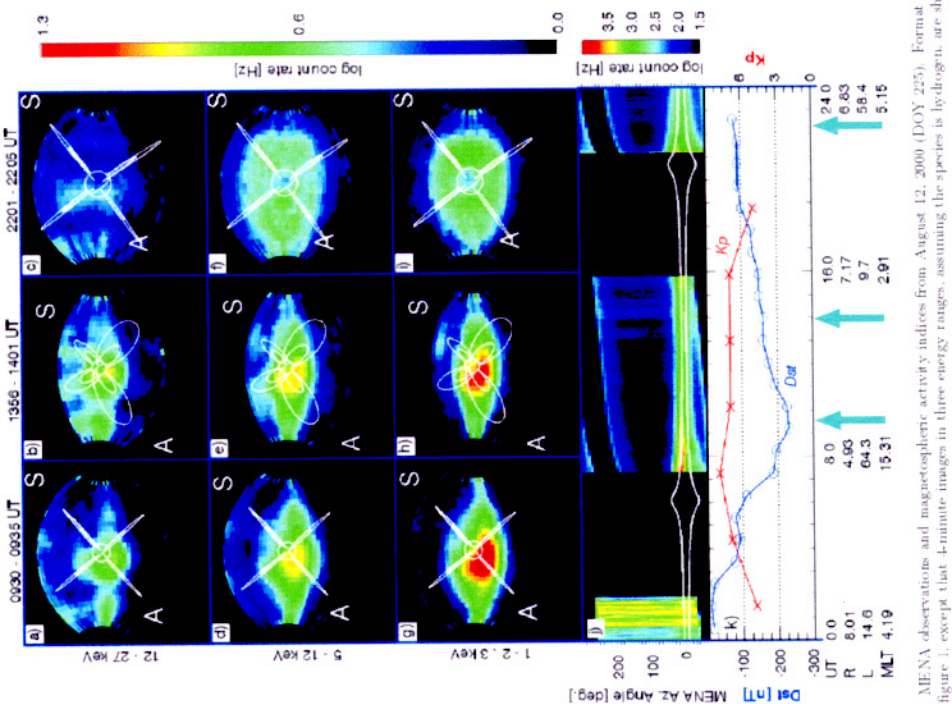


Figure 1. MENA observations and magnetospheric activity indices on July 26, 2000. Bottom panels show quantities plotted versus UT and orbital parameters. Dst (left) and K_p (right) appear in the bottom panel. The second panel from the bottom shows MENA coincidence rates, with IMAGE spin phase plotted on the ordinate and time on the abscissa. Two white lines indicate Earth's limb. Geophysical ENA emissions are ordered with respect to Earth. Detector voltages are reduced in the radiation belts, leaving gaps early on this day, and also between 1200–1600 UT. They are also reduced each spin for sunward viewing. Vertical bands of counts are due to charged particles energetic enough to overcome the electrostatic collimator deflection. The four panels across the top show 4-minute MENA images. Each is annotated with geomagnetic dipole field lines at MLT = 6, 12, 18, and 24 hours and at $L = 4$ and $L = 8$. Noon and midnight field lines are labeled "S" (sunward) and "A" (anti-sunward). The circle at the center of each image indicates Earth. The four images are of ENAs from 5.2–12 keV, assuming the species is hydrogen. Separate color bars to the right provide logarithmic scaling for the coincidence rates and the images.



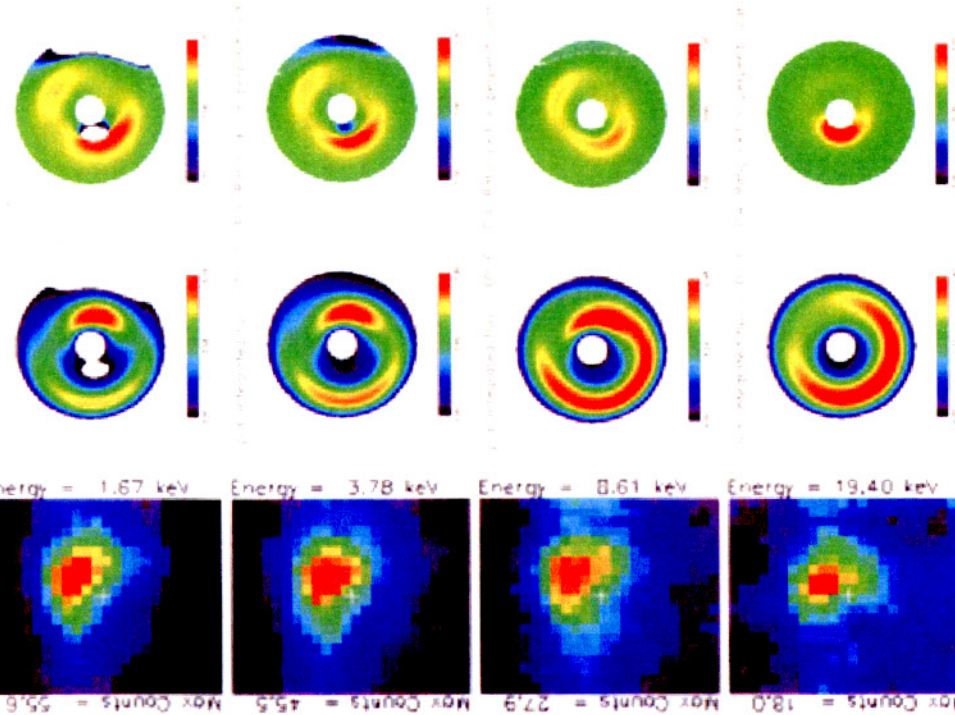
③ Table 1. ENA counts from the dawn (0900–0900), noon (0900–1500), dusk (1500–2100), and midnight (\sim MIN $^+$) 2100–0900 MLT quadrants during storm main phase (0930–0930 UT) and late recovery phase (2200 UT) are compared.

	C_{dawn}	C_{noon}	C_{midnight}
0900 UT	0.05	0.45	0.17
2200 UT	0.90	0.98	1.2

Figure 2. MENA observations and magnetospheric activity indices from August 12, 2000 (DOY 225). Format is similar to that of figure 1, except that 4-minute images in three energy ranges, assuming the species is hydrogen, are shown.

2000/08/12 Event 2

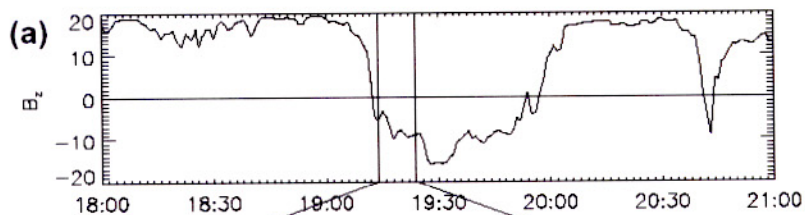
Deconvolution of MENA Image from Aug. 12, 2000 at 9:54:27



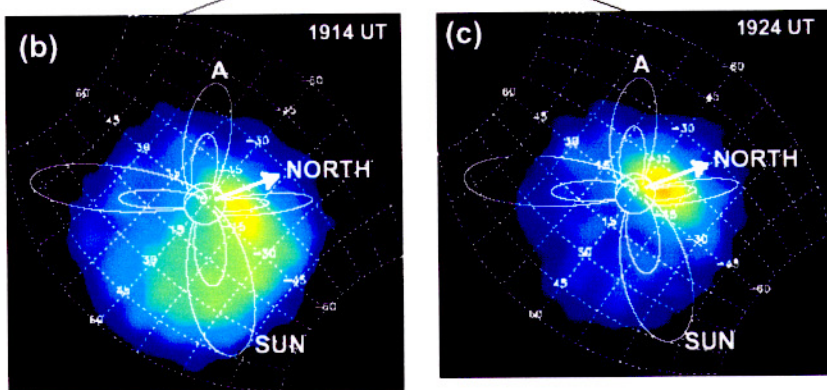
④

Fig. 2 Equatorial pitch angle distributions extracted from MENA images in four different energy intervals. See text for description and interpretation of images.

2000/05/23 Event

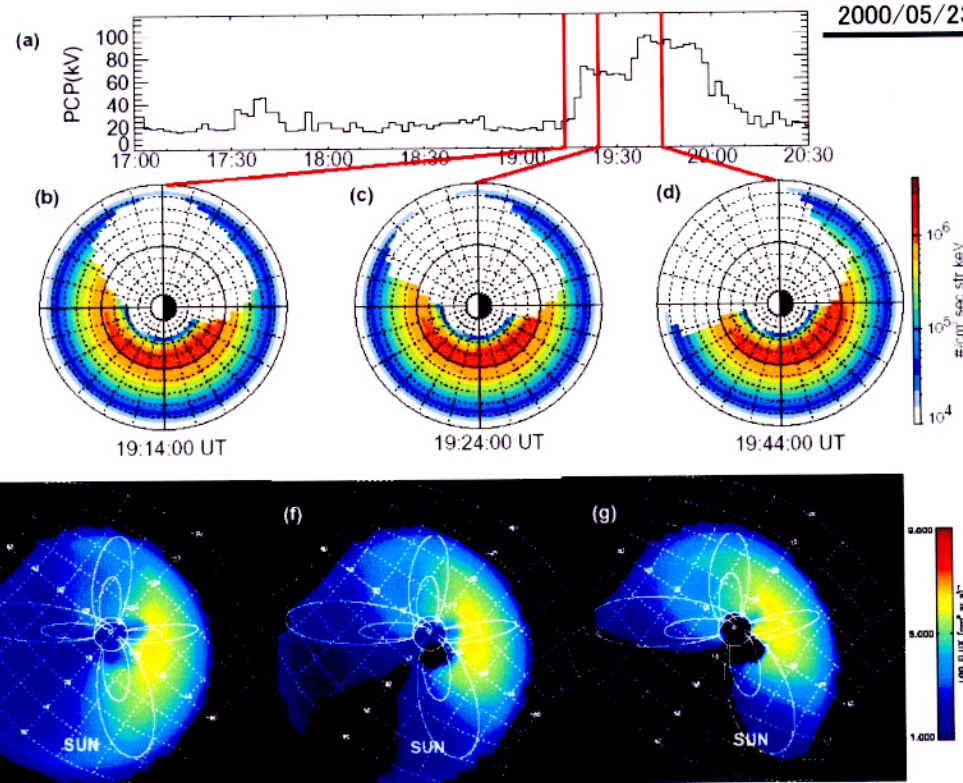


↑ Lagged
↓ 昼側で急激に flux 減少



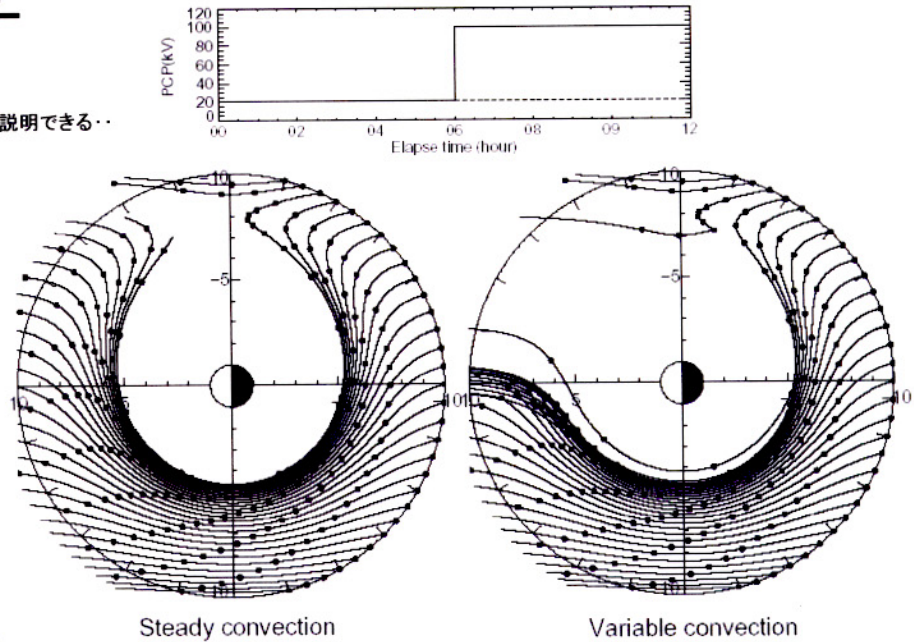
⑤

Plate 1. (a) The interplanetary magnetic field measured by WIND. (b) the observed ENA images (16-50 keV).



2000/05/23 Event 3

Polar Cap Potential の変動で説明できる..



⑤

Figure 1. Drift trajectories of protons with magnetic moment of 0.030 keV in Γ (equatorial pitch angle of 30° (25°) and energy of 30 (5.3) keV at $L = 5$ (10). Left panel shows the trajectories in the steady PCP of 20 kV. Right panel shows the trajectories in the variable convection electric field, that is, the PCP increases from 20 kV to 100 kV at the elapse time of 6 hours. The history of PCP used in the calculation is shown in the top panel.

2000/05/24 Event

Plate 3. ENA images taken from approximately above the north pole. Energy goes down and time goes left to right. Images are taken about 14 hours apart (at 0.27 keV to >100-300 keV). Noontime, the lower eff field line in each image and the approximate equatorial position of Polar (see Figure 4) is marked with a 'P'.
 Sun

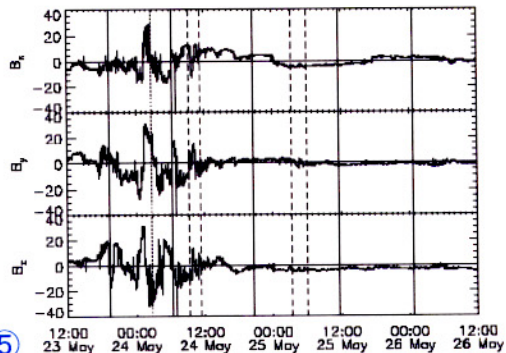
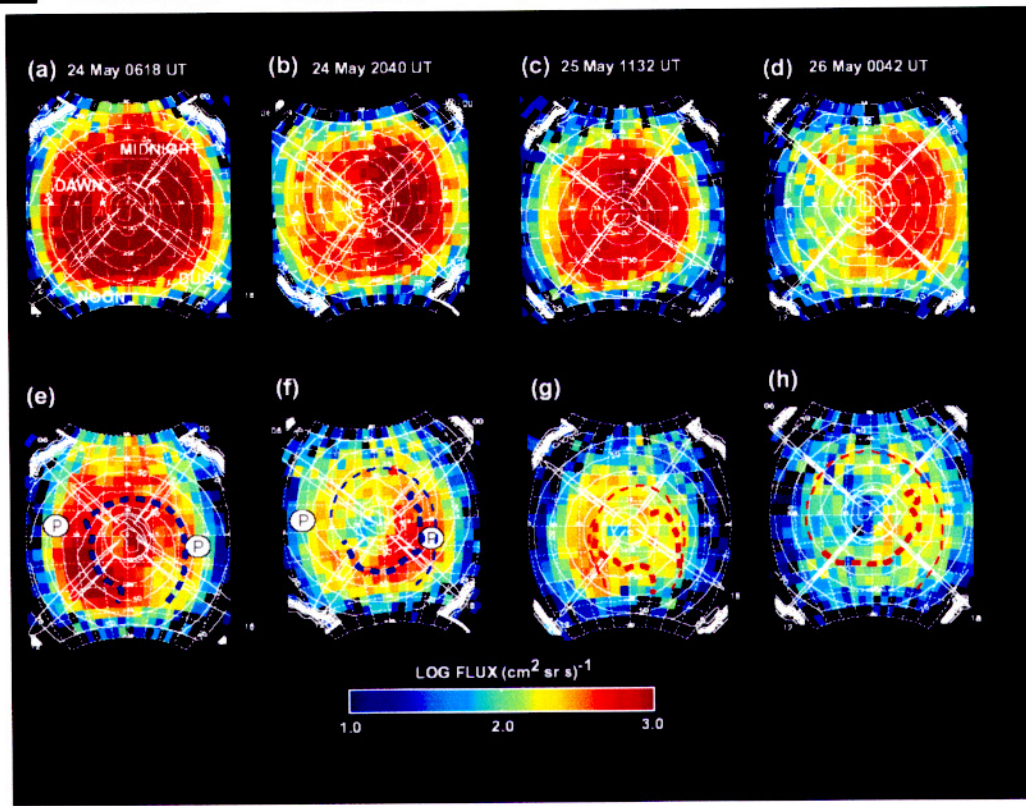


Figure 2. The interplanetary magnetic field. Vertical solid lines are the times of ENA observations. The vertical dotted line is the time of maximum precipitation as seen by the NOAA POES satellite on the duskside and shown in Plate 6. The dashed lines are the times of in-situ measurement by Polar IPS in Figure 4.

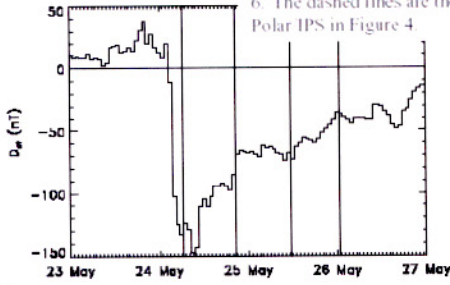


Figure 3. The D_{st} index. Times of the ENA observations are indicated by vertical lines.

2000/05/24 Event 2

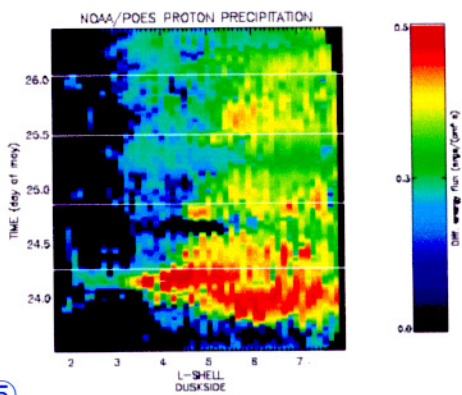


Plate 6. Proton precipitation measured in differential energy flux detected by the NOAA POES satellites. The horizontal white lines mark the times of observations in Plate 3. Strong precipitation for $L < 4$ can be seen early in the beginning of the storm when hot plasma is injected onto low shells.

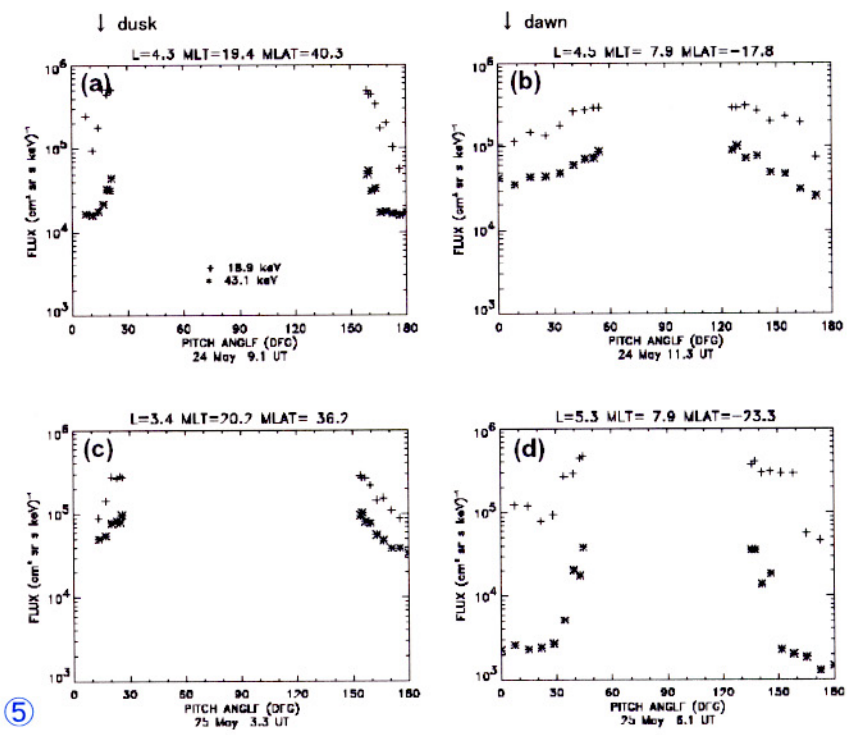


Figure 4. Pitch angle distributions (PAD) mapped to the equator obtained by the imaging proton spectrometer onboard Polar. (a) Duskside for the 24 May 0906 UT at $L=4.3$, (b) dawnside for the 24 May 1120 UT at $L=4.5$, (c) Duskside for the 25 May 0330 UT at $L=3.4$, and (d) dawnside for the 25 May 0606 UT at $L=5.3$. Note that PADs are more peaked around 90° on the duskside for the 24 May and more peaked on the dawn-side for the 25 May.

POLAR / IPS による PAD 観測を反映させてENAを計算・再現

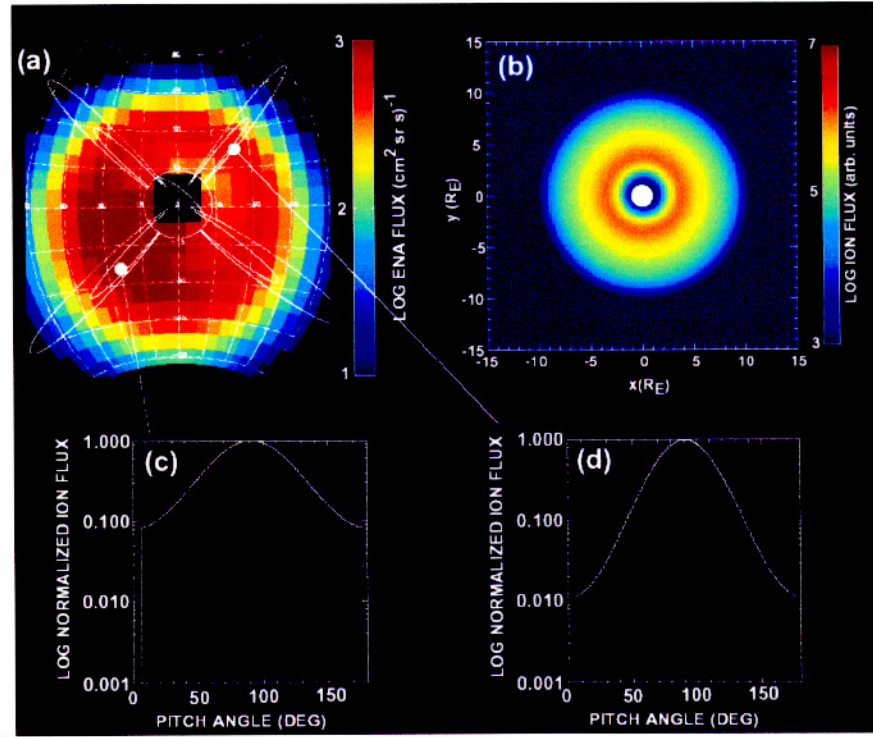
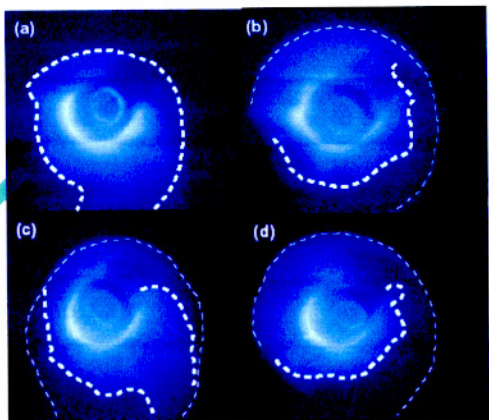
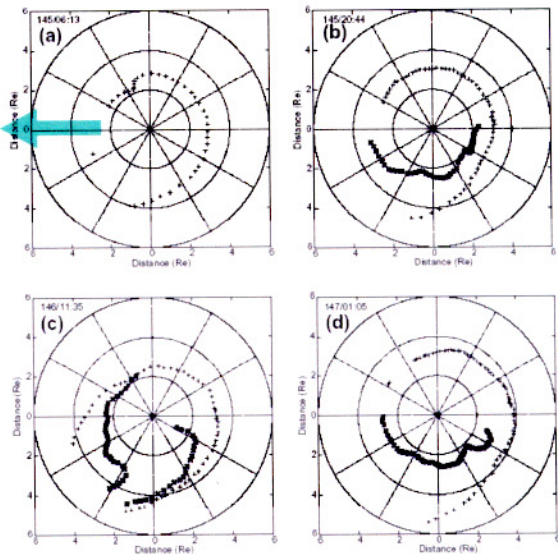


Plate 5. (a) Simulated ENA image for 39-66 keV based on the HENA observations on 24 May 0618 UT shown in Plate 3e. (b) The equatorial proton distribution used to simulate the ENA image. Protons with 90° are shown. Note that the distribution is azimuthally symmetric for this pitch angle. (c) The dayside PAD used in the model and (d) the nightside PAD used in the

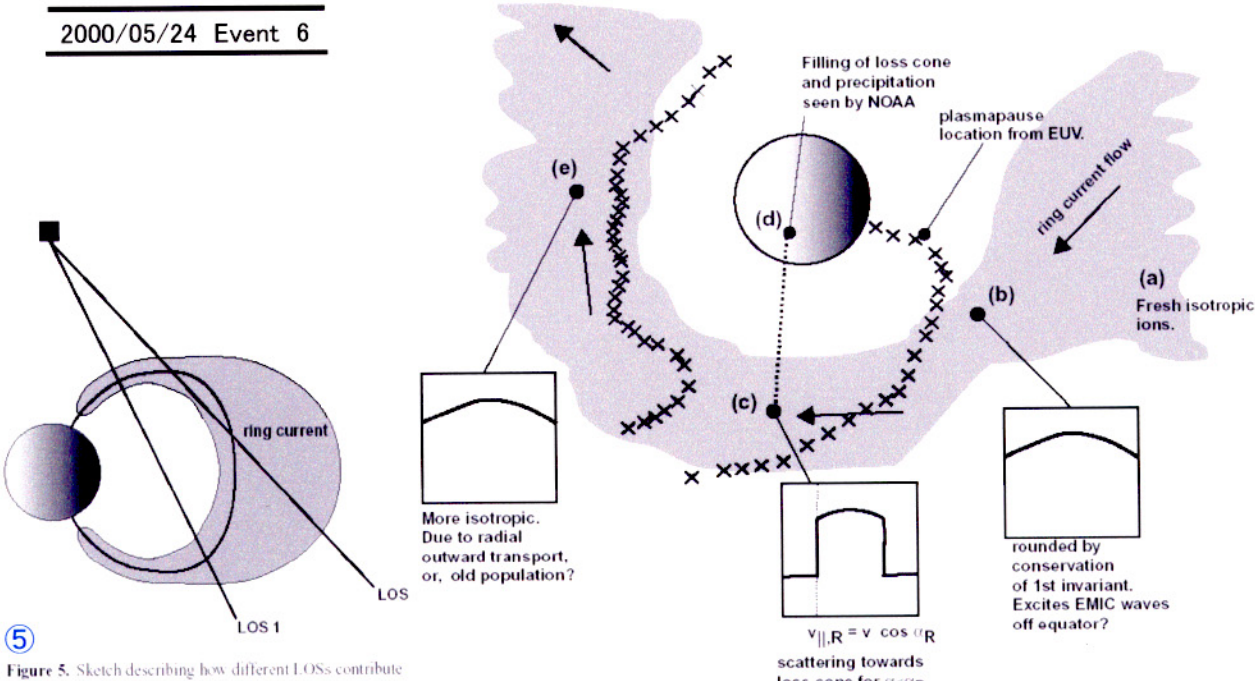
- 矢印 … Sunward
- $a \wedge c$ … dusk 拡大
- $b \wedge d$ … dusk 縮小



⑤ Plate 4. EUV images from the same times as for the columns of Plate 3. Dashed contours mark the gradients in the emission rate found. Thin dashed lines mark that a more diffuse gradient was found and bold, dashed lines mark that a sharp gradient was found. See also Figure 6 for equatorial maps of these contours.



⑤ Figure 6. The corresponding equatorial maps of the tracings of the plasmaspheric gradients in Plate 4. The bold crosses marks the sharp gradients and the thin plusses marks the more diffuse gradients found in the plasmaspheric emissions. Note that the maps are viewed from above the north pole and that noon is to the left in each figure.



⑤ Figure 5. Sketch describing how different LOSs contribute different ENA flux. LOS 1 gives less ENA flux than LOS 2.

⑤ Figure 7. Sketch illustrating a possible scenario for the ring current-plasmasphere interaction. View is from above the north pole.

① Imaging Two Geomagnetic Storms in Energetic Neutral Atoms

D. G. Mitchell¹, K. C. Hsieh², C. C. Curtis², D. C. Hamilton³, H. D. Voss⁴,
E. C. Roelof⁴, P. Cson-Brandt¹

- 2000/07/15-16
 $Dst < -300\text{nT}$
- 2000/06/10
 $Dst \sim -50\text{nT} \rightarrow$ partial ring current

BASTILLE DAY STORM: GLOBAL RESPONSE OF THE TERRESTRIAL RING CURRENT

② P. CSON BRANDT¹, D. G. MITCHELL¹, E. C. ROELOF¹ and J. L. BURCH²

¹The Johns Hopkins University, Applied Physics Laboratory, Maryland, U.S.A.
(e-mail: poutas.brandt@jhuapl.edu)

²Southwest Research Institute, Texas, U.S.A.

Solar Physics 204: 377-386, 2001.
© 2001 Kluwer Academic Publishers. Printed in the Netherlands.

IMF B_z	Dst	Ring Current
-60 nT	main phase	developed Fig.3
negative ~ 0	early recovery	asymmetry Fig.4
positive	recovery	closed ? Fig.5

③ First medium energy neutral atom (MENA) images of Earth's magnetosphere during substorm and storm-time

C.J. Pollock,¹ K. Asamura,² M.M. Balkey,³ J.L. Burch,¹ H.O. Funsten,⁴ M. Grande,⁵ M. Gruntman,⁶ M. Henderson,⁴ J.-M. Jahn,¹ M. Lampton,⁷ M.W. Liemohn,⁸ D.J. McComas,¹ T. Mukai,² S. Ritzau,⁴ M.L. Schattenburg,⁹ E. Scime,³ R. Skoug,⁴ P. Valek^{1,10} and M. Wiest¹

- 2000/07/26 (Fig.1)
 $Dst > -50\text{nT}$, ion injection 2回
- 2000/08/12 (Fig.2)
 $Dst < -230\text{nT}$
main·early recovery \rightarrow partial ring current
late recovery \rightarrow symmetric, closed

④ Initial ion equatorial pitch angle distributions from medium and high energy neutral atom images obtained by IMAGE

J. D. Perez¹, G. Kozlowski², P. Cson-Brandt³, D. G. Mitchell³,
J.-M. Jahn⁴, C. J. Pollock⁴, and X. X. Zhang¹

- Geocorona cross-section model \rightarrow Gruntman [1997,2000]
- Ion pitch angle distribution を cubic B-spline で与え
観測値と合うよう係数を決定するらしい?
- Fig.2 … 分布のピークが、観測では1ヶ所、結果では2ヶ所

Submitted to *J. Geophys. Res.*, 23 March, 2001. Revised 17 July, 2001.

⑤ Global IMAGE/HENA observations of the ring current: Examples of rapid response to IMF and plasmasphere interaction

P. Cson Brandt¹, D. G. Mitchell¹, Y. Ebihara², B. R. Sandel³, E. C. Roelof⁴, J. L. Burch⁴, R. Demajistre¹

- 2000/05/24 Local time distribution of the ring current

- 2000/05/23
Rapid decrease of the dayside fluxes (Plate 1)
 \rightarrow simulation by Ebihara and Ejiri [2000] (Plate 2)
 \rightarrow PolarCap Potential の変動が寄与? (Fig. 1)

ENA (Plate 3) / EUV (Plate 4, Fig. 6)
 \rightarrow ENAの減少とplasmaspheric emissionの増加に相関?

\rightarrow 同時観測 PolarIPS pitch angle distribution (Fig.4)
NOAA/POES proton precipitation (Plate 6)
 \rightarrow simulation (Plate 5)

\rightarrow Fig. 7